Effect of Strain-Induced Martensite on Tensile Properties and Hydrogen Embrittlement of 304 Stainless Steel

YOUNG SUK KIM, SANG HWAN BAK, and SUNG SOO KIM

Room temperature tensile tests have been conducted at different strain rates ranging from 2×10^{-6} to 1×10^{-2}/s on hydrogen-free and hydrogen-charged 304 stainless steel (SS). Using a ferritescope and neutron diffraction, the amount of strain-induced martensite (SIM) has been in situ measured at the center region of the gage section of the tensile specimens or *ex situ* measured on the fractured tensile specimens. The ductility, tensile stress, hardness, and the amount of SIM increase with decreasing strain rate in hydrogen-free 304 SS and decrease in hydrogen-charged one. Specifically, SIM that forms during tensile tests is beneficial in increasing the ductility, strain hardening, and tensile stress of 304 SS, irrespective of the presence of hydrogen. A correlation of the tensile properties of hydrogen-free and hydrogen-charged 304 SS and the amount of SIM shows that hydrogen suppresses the formation of SIM in hydrogen-charged 304 SS, leading to a ductility loss and localized brittle fracture. Consequently, we demonstrate that hydrogen embrittlement of 304 SS is related to hydrogen-suppressed formation of SIM, corresponding to the disordered phase, according to our proposition. Compelling evidence is provided by the observations of the increased lattice expansion of martensite with decreasing strain rate in hydrogen-free 304 SS and its lattice contraction in hydrogen-charged one.

DOI: 10.1007/s11661-015-3198-4

I. INTRODUCTION

IT is well known that bcc martensite is formed in austenitic stainless steels from austenite by plastic deformation, which is termed herein SIM, and that SIM is beneficial in increasing the ductility of austenitic stainless steels, which is a principle of transformation-induced plasticity (TRIP) steel.[1–4] Considering that the bcc martensite is larger in volume than the fcc austenite phase, however, the driving force for nucleation of bcc martensite with a larger volume in fcc austenite remains unclear for around half a century despite the hypotheses proposed by Olson and Cohen[5] and Bogers and Burgers.[6] Besides, it also remains unresolved why SIM increases the ductility and the content of SIM produced during plastic deformation strongly depends upon strain rate and temperature. It has been observed that SIM is formed only at temperatures below the M_d and the higher content of SIM is generated at the lower strain rate. In association with the role of SIM in hydrogen embrittlement (HE) of austenitic stainless steels, there is also a controversy. The first school claims that SIM is detrimental to HE because it acts as a hydrogen path, leading to accumulation of hydrogen at the grain boundary and enhancing HE susceptibility.[7–9] However, Vennett and Ansell[10] observed that exposing a 304 SS with pre-formed martensite to high-pressure hydrogen gas showed no loss in tensile properties upon tensile tests in air, indicating that merely exposing a martensitic or partially martensitic steel to high-pressure hydrogen resulted in no damage. In fact, the tensile properties of austenitic steels are affected not only by SIM formed during tensile tests but also by pre-formed martensite, but the former is beneficial in increasing ductility and the latter is harmful. The second school[11,12] suggests that there is no effect of hydrogen on SIM formation only if the amount of SIM formed in austenitic stainless steels with and without charged hydrogen is compared at the same plastic strain during tensile deformation. In other words, they believe that the less content of SIM formed in hydrogen-charged austenitic steels is caused not by the hydrogen effect but by the decreased plastic strain arising from a ductility loss by hydrogen. The weakness of the latter is that there are no feasible explanations about the ductility loss by hydrogen, the beneficial role of SIM in increasing the ductility of TRIP steels, and a decrease in the yield and tensile stresses by hydrogen, which is called hydrogen softening. In contrast, Shyvaniuk[13] and Mine[14] showed that SIM was suppressed in hydrogen-charged 304 and 316L SS even at the same plastic strain than in hydrogen-free ones and a reverse transformation from SIM to austenite was

YOUNG SUK KIM and SUNG SOO KIM, Principal Researchers, are with the Korea Atomic Energy Research Institute, Daeduk-daero 1045, Yuseong, Daejeon 305-353, Republic of Korea. Contact e-mail: yskim1@kaeri.re.kr SANG HWAN BAK, Graduate Student, formerly with the Korea Atomic Energy Research Institute, is now with Sungkyunkwan University, Suwon, Republic of Korea.

Manuscript submitted May 9, 2015.
Article published online October 20, 2015

enhanced when the strained 304 SS to 45 pct was exposed to hydrogen gas of 100 MPa at 543 K (270 °C) but not when it was exposed to vacuum at 573 K (300 °C), evidently indicating that hydrogen accelerated a reversion transformation from SIM to austenite. Consequently, the role of hydrogen in SIM formation in austenitic stainless steels remains in dispute.

In this work, we demonstrate that the ductility of austenitic stainless steels is related to the amount of SIM generated during plastic deformation irrespective of the presence or absence of hydrogen and that the hydrogen effect is to suppress SIM formation which takes place during plastic deformation, leading to losses in ductility, yield stress and tensile stress, and localized deformation. Specifically, we will show that hydrogen embrittlement in austenitic stainless steels is related to hydrogen-suppressed formation of SIM. Considering that SIM is defined as the bcc phase detected by a ferritescope and neutron diffraction, SIM corresponds to the ferrite phase. To this end, RT tensile tests were conducted on hydrogen-charged and hydrogen-free 304 SS at different strain rates from 2×10^{-6} to 1×10^{-2}/s.

II. EXPERIMENTAL PROCEDURES

The specimen used was as-received (AS) 304 SS plate that was lightly cold-worked according to the measured hardness and microstructural observation. The chemical composition is shown in Table I. Hydrogen charging was carried out using an electrolytic charging method using a 0.5 N H_2SO_4 solution containing 0.25 g/L $NaAsO_2$ at 353 K (80 °C) with a current density of 500 A/m^2 applied for 20 hours. The content of hydrogen charged into the 304 SS was analyzed with a LECO RH-404 analyzer using five different samples. The mean hydrogen content charged in the 304 SS was 51 ± 5 ppm just after hydrogen charging. As soon as hydrogen charging was finished, tensile tests were conducted immediately on the hydrogen-charged 304 SS specimens and later on the hydrogen-free 304 SS samples. To check if martensite is formed during hydrogen charging in 304 SS specimens, the amount of martensite in hydrogen-charged specimens was measured using a ferritescope (Feritscope®-MP30), confirming no martensite formation during hydrogen charging. The amount of SIM was determined by the ferritescope and neutron diffraction. After the ferritescope was calibrated against the five standard samples with the ferrite content ranging from 0.51 to 63.4 pct, the amount of martensite was *ex situ* measured at five different locations at a distance starting from less than 1 mm from the fracture surfaces or in situ measured at the center and its periphery of the gage section of the tensile specimens during tensile deformation as a function of strain. For the latter, the amount of SIM was measured three times at the time interval of either 5-10 seconds at the strain rate of 2×10^{-2}/s or 2-2.5 hours at the slowest strain rate of 2×10^{-6}/s, from which the average value was determined to represent the amount of SIM. Furthermore, using neutron diffraction patterns obtained by a neutron diffractometer at Hanaro, the Korea Atomic Energy Research Institute, the amount of martensite was also determined as the relative ratio of the integral intensity of the (110) ferrite peak over the sum of the integral intensities of the (111) austenite and (110) ferrite peaks. The values determined by neutron diffraction were always higher than those determined by the ferritescope, but both measurements showed the same strain-rate dependence of the amount of SIM. RT tensile tests were conducted at strain rates varying from 2×10^{-6} to 1×10^{-2}/s on duplicate samples of hydrogen-free and hydrogen-charged 304 SS except at the slowest strain rate of 2×10^{-6}/s, where a single specimen was used. The tensile properties of 304 SS were taken as the average of two measured values. The 304 SS tensile specimens were rod shaped with a diameter of 4 mm and a gage length of 25.4 mm. Changes in the lattice parameters of austenite and martensite in 304 SS during RT tensile tests were determined using neutron diffraction by a change in the peak positions, and their confidence level was $\Delta d/d \cong 0.004$ pct.

III. RESULTS

The tensile properties of 304 SS strongly depended on strain rate and charged hydrogen. As shown in Figure 1, hydrogen-free 304 SS exhibited a significant increase in tensile stress and ductility and a slight decrease in yield stress with decreasing strain rate. This strain-rate dependence of the tensile properties of hydrogen-free 304 SS agrees perfectly with the previous observations in 301 SS,[15–17] Fe-Ni-C,[18,19] and 304 or 304L SS.[20–25] In hydrogen-charged 304 SS, however, hydrogen had little effect on the yield stress except at the slowest strain rate of 2×10^{-6}/s leading to a very slight decrease in the yield stress but a significant decrease in tensile stress and ductility at all strain rates. However, the loss in tensile stress and ductility by hydrogen in hydrogen-charged 304 SS showed a strong strain-rate dependence (Figures 1a and b). In other words, the largest loss in tensile stress and ductility by hydrogen occurred at the slowest strain rate of 2×10^{-6}/s. This hydrogen softening corresponding to a decrease in the flow stress by hydrogen has also been observed in 316L SS,[26] iron,[27,28] and mild steels.[29] Figure 2 shows the fracture surfaces of hydrogen-free and hydrogen-charged 304 SS after RT tensile tests. The dominant fracture mode of

Table I. Chemical Composition of 304 Stainless Steel

Composition	Cr	Ni	Mo	C	Si	Mn	P	S	N	Co	Cu	Fe
304 SS	18.17	8.03	0.11	0.043	0.46	1.04	0.001	0.04	0.047	0.12	0.18	bal

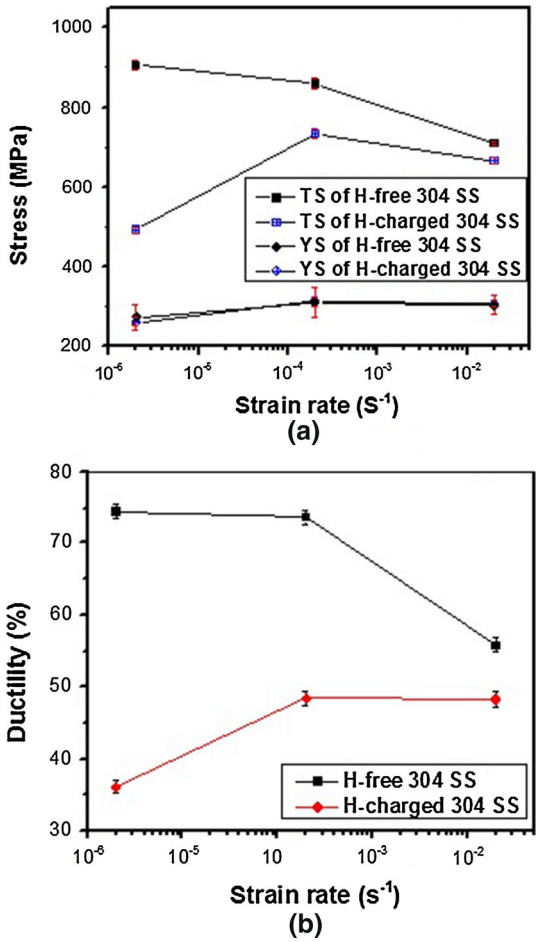

Fig. 1—Strain-rate dependence of room-temperature tensile properties of hydrogen-free and hydrogen-charged 304 SS: (*a*) yield and tensile stresses and (*b*) ductility.

the former was uniformly ductile fracture with fine dimples whose size seems to change little with decreasing strain rate, as shown in Figure 2(a). The fracture mode of the latter changed significantly with decreasing strain rate, *i.e.*, it showed uniformly ductile fracture with fine dimples at 2×10^{-2}/s but localized brittle fracture of rectilinear shape parallel to each other at slower strain rates below 2×10^{-2}/s (Figures 2b and c). Thus, it is evident that hydrogen promoted localized brittle fracture in hydrogen-charged 304 SS, which became more striking with decreasing strain rate, and that the slower the strain rate, the larger the difference in the fracture mode between the hydrogen-free and hydrogen-charged 304 SS.

To show the strain-rate dependence of SIM formation during the tensile tests, the amount of SIM was determined in hydrogen-free and hydrogen-charged 304 SS deformed at different strain rates by neutron diffraction and a ferritescope. As shown in Figure 3, the amount of SIM increased with decreasing strain rate in hydrogen-free 304 SS but decreased in the hydrogen-charged one. Note that although the amount of SIM determined by neutron diffraction was 2 to 3 times higher than that by the ferritescope in hydrogen-free and hydrogen-charged 304 SS, respectively, the strain-rate dependences of the amount of SIM formed in hydrogen-free and hydrogen-charged 304 SS were observed to be similar, irrespective of whether the amount of SIM was determined by neutron diffraction or the ferritescope. Talonen[20,21] also used a correction factor of 1.7 multiplied to the ferritescope reading to calculate the actual martensite content, which was obtained by comparing X-ray diffraction results and those by the ferritescope. Surprisingly, the amount of SIM formed in 304 SS at 3×10^{-4}/s, which was determined by Talonen,[20] was 66-67 pct, which agrees perfectly with that at 2×10^{-4}/s, corresponding to 68 pct, when determined by neutron diffraction, as shown in Figure 3 and Table II.

The increased amount of SIM with decreasing strain rate in hydrogen-free 304 SS coincides perfectly with the previous observations.[15–25] However, the amount of SIM formed upon tensile tests was lower in the hydrogen-charged 304 SS than in the hydrogen-free one, independent of the strain rate, as shown in Figure 3. This observation indicates that hydrogen suppressed SIM formation in 304 SS during the tensile tests. This hydrogen-suppressed formation of SIM has also been observed in Type 304 SS with pre-charged hydrogen during tensile tests at RT[13] or during high-pressure torsion,[14] in 301 SS tensile tested in 108 kPa H_2 gas,[9] in 316 SS deformed in a hydrogen gas environment,[30] in 301/302 SS after fatigue tests in 1 atm H_2 gas,[31] and in austenitic stainless steels during cathodic hydrogen charging.[32] The most significant decrease in the amount of SIM by hydrogen occurred at the slowest strain rate of 2×10^{-6}/s. Considering the hypothesis of the second school that hydrogen has no effect of the amount of SIM, in situ measurements of SIM were conducted in hydrogen-charged and hydrogen-free 304 SS during tensile tests at different strain rates ranging from 2×10^{-6} to 2×10^{-2}/s using a ferritescope. As shown in Figure 4, the amount of SIM formed in 304 SS during tensile tests was observed to be dictated by strain rate and hydrogen: the lesser amount of SIM was formed in hydrogen-charged 304 SS than in hydrogen-free one, irrespective of the magnitudes of strain and strain rate. In other words, hydrogen suppressed SIM formation in 304 SS even at the same plastic strain. Furthermore, hydrogen-suppressed formation of SIM was significantly enhanced at the lowest strain rate of 2×10^{-6}/s when compared to that at the higher strain rate of 2×10^{-2}/s. Note that the observations of Figure 4 excellently agree with those of Shyvaniuk[13] and Mine[14] that the less amount of martensite was formed in hydrogen-charged 304 and 316L SS when compared to that in hydrogen-free ones, irrespective of the magnitude of strain.

To show a correlation between the amount of SIM and the tensile properties of 304 SS, the ductility, strain hardening, and tensile stress of hydrogen-free and hydrogen-charged 304 SS were described as a function of the amount of SIM, as shown in Figure 5. Note that the strain hardening shown in Figure 5 is denoted as the ratio of a stress increment from the yield stress to the tensile stress over the yield stress or (TS-YS)/YS where TS and YS are the tensile and yield stresses of 304 SS, respectively. All tensile properties of hydrogen-free and

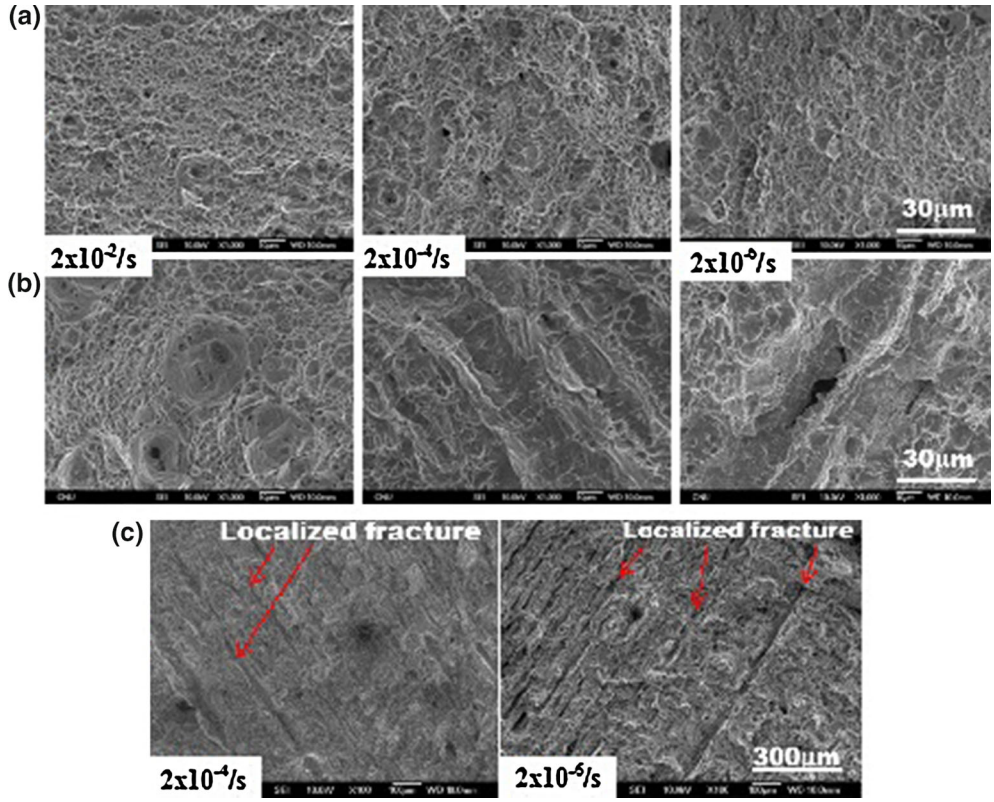

Fig. 2—Fracture surfaces of (*a*) hydrogen-free and (*b*) hydrogen-charged 304 SS with strain rate. (*c*) Lower magnification photos of (b) deformed at 2×10^{-4} and 2×10^{-6}/s, showing localized rectilinear fracture.

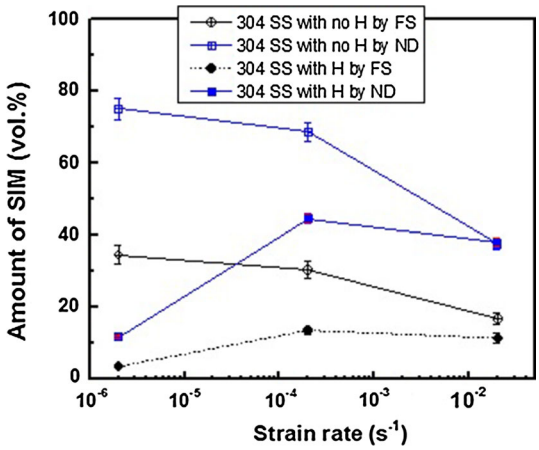

Fig. 3—The amount of strain-induced martensite with strain rate formed during tensile tests in hydrogen-free and hydrogen-charged 304 SS determined primarily by a ferritescope (FS) and neutron diffraction (ND).

hydrogen-charged 304 SS showed a strong dependence on the amount of SIM formed during the tensile tests: the ductility, strain hardening (Figure 5a), and tensile stress (Figure 5b) increased linearly with the amount of SIM independent of the presence of hydrogen. Specifically, SIM was beneficial in increasing the ductility, strain hardening, and tensile stress of 304 SS independent of the presence of hydrogen, which is consistent with the so-called TRIP effect in which SIM transformation leads to an increase in ductility and tensile stress.[2–4,18–25,33,34] Given these correlations of Figure 5 and hydrogen-suppressed formation of SIM shown in Figures 3 and 4, it is evident that the lower ductility, strain hardening, and tensile stress of hydrogen-charged 304 SS are related to the decreased amount of SIM formation during the tensile tests in the presence of hydrogen. In other words, hydrogen-suppressed SIM formation is the origin of the loss in ductility, strain hardening, and tensile stresses, *i.e.*, hydrogen softening in hydrogen-charged 304 SS. In short, we demonstrate that hydrogen embrittlement and softening of 304 SS are related to hydrogen-suppressed SIM formation.

To show if a change in the lattice parameters of hydrogen-free and hydrogen-charged 304 SS occurred during the RT tensile tests, the *d*-spacing of austenite and martensite was determined as a function of strain rate, using neutron diffraction. Note that the percent variation in the *d*-spacing is termed a fractional change in the peak positions of the austenite (111) and martensite (110) planes before and after the tensile tests. Especially, for hydrogen-charged 304 SS, the lattice parameters of the austenite (111) and martensite (110) before and after tensile tests were determined from the grip parts and the gage sections, respectively, of the tensile specimens after tensile tests. As shown in Figure 6(a), the *d*-spacing of the martensite (110) formed in the hydrogen-free 304 SS increased with decreasing strain rate, indicating that the martensite

Table II. Hardness and the Amount of Strain-Induced Martensite (SIM) of Hydrogen-Free and Hydrogen-Charged 304 SS with Strain Rate upon RT Tensile Deformation as Compared to the As-Received 304 SS

			RT tensile deformation		
			Strain rate (1/s)		
Specimen	Properties of 304 SS	As-received	2×10^{-6}	2×10^{-4}	2×10^{-2}
H-free 304 SS	hardness (Hv)	261	464	417	360
	amount of SIM (percent)	0	75	68	38
H-charged 304 SS	hardness (Hv)	247	311	381	368
	amount of SIM (percent)	0	12	45	38

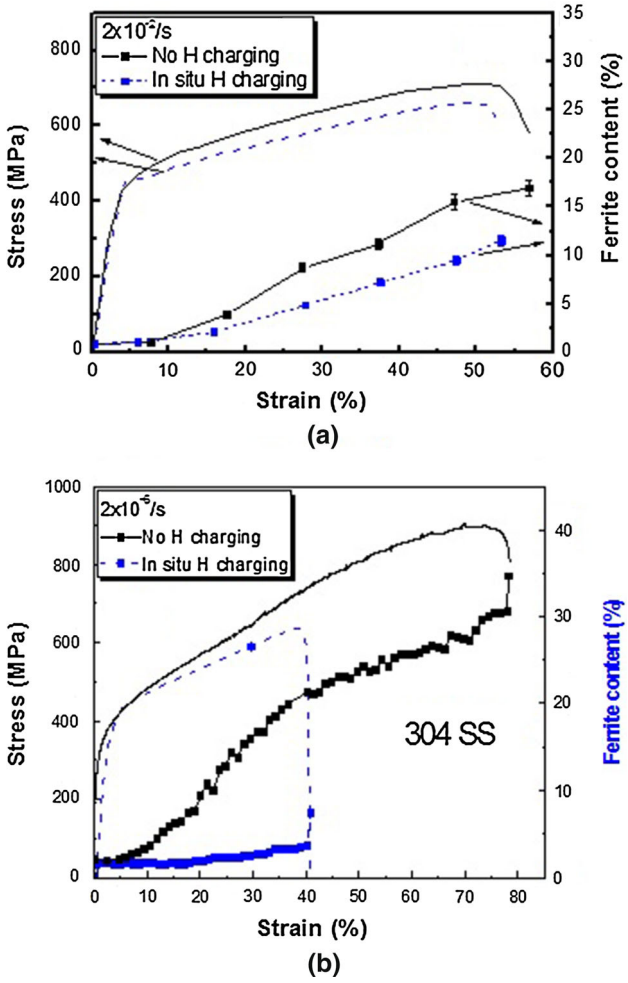

Fig. 4—Stress–strain curves of 304 SS and the amount of SIM formed at different strain rates under in situ hydrogen charging conditions: (*a*) 2×10^{-2}/s and (*b*) 2×10^{-6}/s.

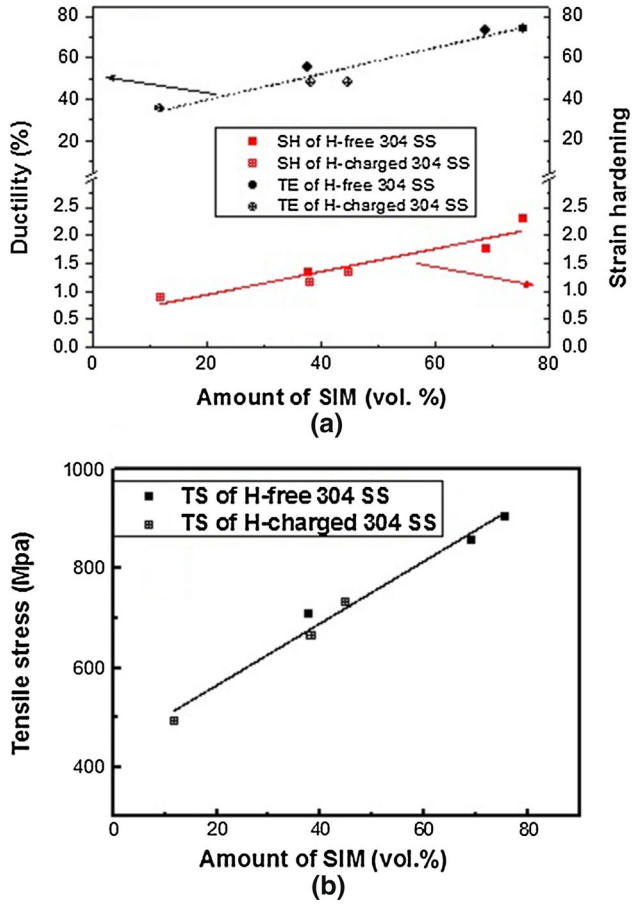

Fig. 5—Linear dependences of (*a*) the ductility and strain hardening and (*b*) the tensile stress of 304 SS on the amount of SIM formed during room-temperature tensile tests, irrespective of the presence or absence of hydrogen.

showed a lattice expansion during the tensile tests and the magnitude of the lattice expansion increased with decreasing strain rate. In contrast, the d-spacing of the austenite (111) plane in the hydrogen-free 304 SS was decreased slightly with decreasing strain rate, revealing that a little lattice contraction occurred in the austenite. The increased lattice expansion of martensite and lattice contraction of austenite with decreasing strain rate shown in Figure 6(a) agree perfectly with the observations of Tao[33] and Oliver[35] that austenite and martensite in TRIP steels showed lattice contraction and expansion, respectively, upon RT tensile tests the degree of which increased with increasing martensite volume fraction. In the hydrogen-charged 304 SS, as shown in Figure 6(b), however, the martensite (110) showed a lattice contraction during the tensile tests which is in contrast with its lattice expansion in the hydrogen-free 304 SS (Figure 6a). The *d*-spacing of the austenite (111) plane showed little change with decreasing strain rate.

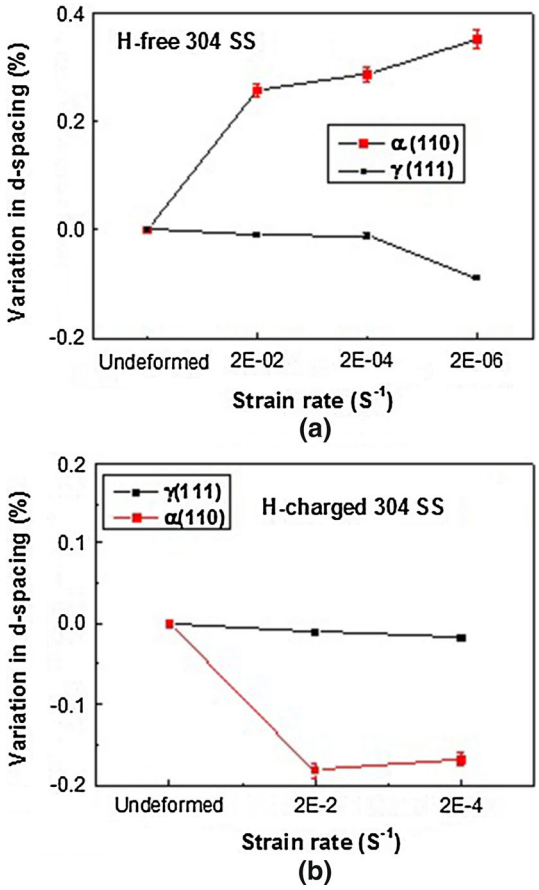

Fig. 6—Variations of *d*-spacing of martensite and austenite in (*a*) hydrogen-free and (*b*) hydrogen-charged 304 SS during the RT tensile tests.

IV. DISCUSSION

A. *Strain-Rate Dependence of Tensile Properties of Hydrogen-Free 304 SS*

Hydrogen-free 304 SS showed a strain-rate dependence of the tensile properties: with decreasing strain rate, hydrogen-free 304 SS showed a decreased yield stress and increased ductility and tensile stress, as shown in Figure 1. Furthermore, by correlating their tensile properties to the amount of SIM in each, as shown in Figure 5, the strain-rate dependence of the tensile properties of hydrogen-free 304 was observed to be related to the amount of SIM formed during tensile tests. The above observations agree with the results reported by other workers.[2–4,15–25] Thus, SIM formation during tensile tests is beneficial in increasing the tensile stress, ductility, and strain hardening of austenitic stainless steels.

The cause of the strain-rate dependence of the amount of SIM formed in austenitic stainless steels, as shown in Figures 3 and 4, has remained unresolved hitherto although a higher temperature rise in the specimen at a higher strain rate was suggested to be part of the cause by Bressanelli[15] and Hecker.[23] However, considering Tamura's observations[18,19] that a similar strain-rate dependence of the amount of SIM occurred in austenitic steels upon tensile tests in gas as well as in liquid where little temperature rise occurred due to fast cooling, it seems that a strain-rate dependence of the amount of SIM in austenitic stainless steels is related not to a temperature rise at a higher strain rate but to something else. Similar remarks have also been made by Tamura.[18] Supportive evidence of SIM formation in austenitic stainless steels during tensile tests is a hardness change in austenitic stainless steels with strain rate. As shown in Table II, the hardness of hydrogen-free 304 SS increased with decreasing strain rate owing to the negative strain-rate dependence of the amount of SIM formed during the tensile tests shown in Figure 4. These observations show that SIM has a higher hardness than austenite. Note that the lower hardness of hydrogen-charged 304 SS agrees perfectly with Mine's observation.[14] However, it is difficult to understand why a larger amount of hard SIM led to a higher ductility, as shown in Table II and Figure 5.

B. *Hydrogen-Suppressed Formation of SIM in Hydrogen-Charged 304 SS*

As shown in Figure 1, the presence of hydrogen resulted in a decrease in the tensile stress, *i.e.*, hydrogen softening, and a ductility loss in 304 SS when compared to the hydrogen-free samples. Furthermore, hydrogen suppressed the formation of SIM in hydrogen-charged 304 SS, resulting in the formation of less SIM during tensile tests, as shown in Figures 3 and 4. Considering the beneficial role of SIM in the tensile properties of austenitic stainless steels in hydrogen-free 304 SS (Figure 5), ductility losses and hydrogen softening in the hydrogen-charged 304 SS are related to the hydrogen-suppressed formation of SIM. This hydrogen-suppressed formation has also been observed during RT tensile deformation or high-pressure torsion in hydrogen-charged 304 SS after exposure to hydrogen gas pressure of 100 MPa at 543 K (270 °C) for 100 hours.[13,14] Hydrogen-suppressed formation of SIM in 304 SS was observed more significantly at the slowest strain rate, as shown in Figures 3 and 4, providing definitive evidence that it occurred due to the hydrogen effect even at the same plastic strains. The lowest content of SIM formed at the slowest strain rate of 2×10^{-6}/s in hydrogen-charged 304 SS resulted in the lowest ductility of 304 SS, as shown in Figures 1, 4 and 5. It is worthy of noting that the strain-rate dependence of ductility of 304 SS was negative in hydrogen-free sample but positive in hydrogen-charged one.

Given that SIM is harder than austenite[14] and that hydrogen suppresses the formation of SIM in hydrogen-charged 304 SS as shown in Figures 3 and 4, hydrogen-charged 304 SS should have a lower hardness than hydrogen-free ones. As expected, the former indeed exhibited lower hardness than the latter, as shown in Table II, which provides compelling evidence that hydrogen suppressed the SIM formation. Note that the lower hardness of hydrogen-charged 304 SS agrees perfectly with Mine's observation.[14] Thus, the localized brittle fracture of hydrogen-charged 304 SS when compared to that of the hydrogen-free versions, as

shown in Figure 2, is related to the lower amount of SIM formed during tensile deformation owing to the hydrogen-suppressed formation of SIM. Consequently, we demonstrate that this hydrogen-suppressed formation of SIM is the cause of hydrogen embrittlement and hydrogen softening in austenitic stainless steels.

C. *The Nature of Strain-Induced Martensite (SIM)*

Given the observations that SIM is beneficial in increasing the ductility of austenitic stainless steels, some workers[18,19,36,37] proposed that SIM would delay the formation of necking by the $\gamma \rightarrow \alpha$ transformation during tensile deformation, promoting more uniform deformation. This hypothesis is very similar to the proposed mechanism explaining the enhanced ductility of TRIP steels.[36] If this delaying mechanism is valid, 310 SS with no SIM formation during tensile tests should not show a strain-rate dependence of ductility. Given Form and Baldwin's observation[38] that 310 SS with no $\gamma \rightarrow \alpha$ transformation showed a similar strain-rate dependence to that of 304 SS, they claim that the strain-rate dependence of ductility in austenitic stainless steels may not be wholly related to the $\gamma \rightarrow \alpha$ transformation. Consequently, the hypothesis that the $\gamma \rightarrow \alpha$ transformation may suppress the formation of necking, leading to a higher ductility, may be at least partly invalid.

Form and Baldwin[38] observed that the strain-rate dependence of ductility occurred not only in 304 SS with SIM formation but also in 310 SS without it. Furthermore, it is well known that the disordered phase has a lower yield stress, and a higher ductility and strain hardening, than the ordered phase.[39–41] By correlating Form and Baldwin's observations and RT tensile properties of the disordered phase, it is suggested that SIM formed in 304 SS would correspond to the disordered phase which would also be induced in 310 SS by the passage of dislocations during tensile tests at RT.[42–44] Disordered phase formation arising from the destruction of the ordered phase by moving dislocations is termed strain-induced disordering (SID),[45] and the disordered phase is formed predominantly by plastic deformation in metals at low temperatures where the rate of disordering exceeds the rate of strain-induced ordering (SIO),[46] *i.e.*, the rate of ordering. Hence, a linear increase in the ductility and strain hardening of 304 SS with increasing amount of SIM despite a hard phase, as shown in Figure 5, suggests that SIM corresponds to the disordered phase. Compelling evidence is the observations of Figure 6(a) that the martensite showed a lattice expansion whose magnitude increased with decreasing strain rate. Furthermore, considering that the degree of lattice expansion is related to the amount of the disordered phase,[47] the increased lattice expansion of the martensite with decreasing strain rate, as shown in Figure 6(a), indirectly demonstrates that a higher amount of the disordered phase, *i.e.*, SIM, is formed with decreasing strain rate, as evidenced by the observations of Figures 3 and 4. A correlation of the amount of the disordered phase and the degree of lattice expansion results from the fact that the disordered phase has a higher volume than the ordered phase[47] as with a higher volume of the disordered liquid than that of the ordered solid.

Conversely, the hydrogen-suppressed formation of SIM, shown in Figure 3 and 4, corresponds to hydrogen-suppressed disordering or hydrogen-enhanced ordering, leading to lattice contraction. Compelling evidence is the higher lattice contraction of the martensite (110) with the lower strain rate in hydrogen-charged 304 SS shown in Figure 6(b). Given that the lattice contraction is caused by ordering,[47–49] as with solidification shrinkage occurring in the disordered liquid-ordered solid phase transition, a lattice contraction of the martensite (110) by hydrogen corresponds to hydrogen-enhanced ordering. This rationale perfectly agrees with our observation[49] in Alloy 600 and the previous observations in Pd_3Mn,[50] pure Ni,[51] and Fe[52] that hydrogen enhances ordering, consistently validating our proposition. Further support is provided by Shyvaniuk's observation[13] that hydrogen enhances the reverse transformation from martensite to austenite even without plastic deformation, corresponding to hydrogen-suppressed formation of martensite, *i.e.*, the disordered phase. Consequently, a ductility loss by hydrogen is due to suppressed formation of the disordered phase by hydrogen or hydrogen-suppressed formation of SIM. In view of this rationale, the negative and positive strain-rate dependences of the tensile stress and ductility of hydrogen-free and hydrogen-charged 304 SS, respectively, as shown in Figure 1, are related to the disordering rate in the former and the ordering rate by hydrogen in the latter, respectively, accompanied during tensile tests at RT. Therefore, considering that either disordering or ordering is related to the diffusion of atoms, the rate of ordering or disordering will be enhanced with decreasing strain rate. This rationale can explain the negative and positive strain-rate dependences of the amount of SIM in hydrogen-free and hydrogen-charged 304 SS, respectively, as shown in Figures 3 and 4. However, if a temperature rise is accompanied during tensile tests, the increased temperature suppresses SID and instead enhances SIO, suppressing the formation of the disordered phase or SIM, as suggested by Bressanelli[15] and Tamura.[18,19] Given this rationale, the M_d temperature above which SIM is suppressed is a critical temperature where the disordered phase corresponding to SIM is suppressed due to SIO. Thus, the positive strain-rate dependence of elevated-temperature tensile properties of austenitic stainless steels would occur owing to SIO as with that of RT tensile properties of hydrogen-charged 304 SS, as shown in Figure 1. Given the characteristics of SIO occurring at high temperature, which leads to a lower ductility, enhanced SIO in austenitic Ni-Cr-Fe alloys with decreasing strain rate would lead to an enhanced ductility loss and intergranular cracking susceptibility with decreasing strain rate in unirradiated and irradiated 304 SS, as observed by Ehrnsten[53] and Manahan,[54] respectively. In other words, the strain-rate dependences of mechanical properties always occur in all metals, although the strain rate effects differ depending on

whether SIO or SID becomes predominant at the operating conditions to which they are exposed.

The above discussions assume that SIM is the disordered phase of the bcc structure. Considering that the ordered phase to be formed in Fe-based steels is DO_3 Fe_3Ni[55–60] and the disordered phase of the ordered DO_3-Fe_3Ni is bcc,[61,62] SIM would be the disordered bcc-Fe_3Ni generated by the destruction of short-range ordered DO_3-Fe_3Ni by moving dislocations, which is termed the SID transformation. Specifically, the SIM would be a nickel-rich disordered phase with the nickel content increasing to around 25 at. pct when compared to that of the austenite phase. Supportive evidence is provided by the observations of Saha *et al.*'s[63] that the nickel-rich clusters in retained austenite contain up to 30 at. pct Ni. Prokoshkin[55] and Menshikov[64] also observed short-range order of Fe_3Ni with about 30 pct Ni in Fe-Ni austenite alloys for quenching temperatures up to 1373 K (1100 °C) and higher. Superstructure Fe_3Ni with a DO_3 structure was observed to be formed upon heating an Fe-29 at. pct Ni alloy consisting of austenite only, which was transformed to another ordered phase with a B2 structure at 873 K (600 °C) with the second transformation from B2 to disordered bcc α phase at 1073 K (800 °C).[60] Furthermore, Post and Eberly[65] also claimed that SIM would be chromium nickel ferrite. Just recently, using atom probe tomography and small-angle neutron scattering, we have successfully observed the presence of nickel-rich clusters in solution-annealed (SA) 316 SS and aged SA 316 SS at 673 K (400 °C) for over 1000 hours which has the composition of $(Fe,Cr)_3Ni$. These results will be published somewhere else.

Considering that the disordered phase formed in austenitic stainless steels strongly depends on the chemical composition of the austenite phase, and that the chemical composition of 310 SS is quite different from that of 304 SS, the disordered phase formed in 310 SS seems to have a different chemical composition from SIM formed in 304 SS. Thus, the reason why no SIM is formed in 310 SS during tensile tests at RT is related to the formation of the disordered phase with different chemical composition from that of SIM.

V. CONCLUSIONS

Negative and positive strain-rate dependences of RT tensile properties are observed in hydrogen-free and hydrogen-charged 304 SS, respectively; the ductility, tensile stress, hardness, and SIM content increase with decreasing strain rate in hydrogen-free 304 SS but decrease in hydrogen-charged 304 SS. By correlating the amount of SIM formed during the tensile tests with their tensile properties, we show that the ductility, strain hardening, and tensile stress of hydrogen-free 304 SS are dictated by the amount of SIM formed during the tensile tests, irrespective of the presence of hydrogen. In other words, SIM is observed to be beneficial in increasing the ductility, tensile stress, and strain hardening and leading to ductile fracture with fine dimples in hydrogen-free 304 SS. In contrast, hydrogen suppresses SIM formation in hydrogen-charged 304 SS, leading to significant losses in ductility, tensile stress, and strain hardening and to localized brittle fracture, which is augmented with decreasing strain rate. Given the beneficial role of SIM, this hydrogen-suppressed formation of SIM is the cause of a ductility loss by hydrogen, *i.e.*, hydrogen embrittlement, in hydrogen-charged 304 SS. Consequently, we demonstrate that hydrogen embrittlement of austenitic stainless steels is related to the hydrogen-suppressed formation of SIM. Considering that SIM increases the ductility and decreases the yield stress of austenitic stainless steels, we propose that SIM is a disordered bcc phase ($(Fe,Cr)_3Ni$) created by the destruction of short-range ordered DO_3-$(Fe,Cr)_3Ni$ by moving dislocations, which can account for strain-rate dependences of tensile properties of hydrogen-free and hydrogen-charged 304 SS. Compelling evidence is provided by the observations of a change in the lattice parameter of martensite with strain rate in hydrogen-free and hydrogen-charged 304 SS during the RT tensile tests: the lattice expansion with decreasing strain rate increases in hydrogen-free 304 SS and its lattice contraction occurs in hydrogen-charged 304 SS. Thus, the hydrogen-suppressed formation of SIM corresponds to hydrogen-enhanced ordering, which agrees with the previous observations.

ACKNOWLEDGMENTS

This work was carried out as a part of the Nuclear R&D Program funded by the Korean Ministry of Science, ICT and Future Planning. Special thanks are due to S.S. Lee who conducted neutron diffraction experiments at KAERI and to H.M. Choe who thoroughly reviewed the manuscript.

REFERENCES

1. V.F. Zackay, E.R. Parker, D. Fahr, and R. Busch: *Trans. ASM*, 1967, vol. 60, pp. 252–59.
2. W.W. Gerberich, P.L. Hemmings, and V.F. Zackay: *Met. Trans.*, 1971, vol. 2, pp. 2243–53.
3. W.W. Gerberich, P.L. Hemmings, M.D. Merz, and V.F. Zackay: *Trans. Techn. Notes*, 1968, vol. 61, pp. 843–47.
4. P.C. Maxwell, A. Goldberg, and J.C. Shyne: *Metall. Trans.*, 1974, vol. 5, pp. 1319–24.
5. G.B. Olson and M. Cohen: *J. Less Common Met.*, 1972, vol. 28, pp. 107–18.
6. A.J. Bogers and W.G. Burgers: *Acta Met.*, 1964, vol. 12, pp. 255–61.
7. G. Han, J. He, S. Fukuyama, and K. Yokogawa: *Acta Mater.*, 1998, vol. 46, pp. 4559–70.
8. C.L. Briant: *Met. Trans. A*, 1979, vol. 10, pp. 181–89.
9. T.P. Perng and C.J. Altstetter: *Met. Trans. A*, 1987, vol. 18A, pp. 123–34.
10. R.M. Vennett and G.S. Ansell: *Trans. ASM.*, 1967, vol. 60, pp. 242–51.
11. J.H. Ryu, Y.S. Chun, C.S. Lee, H.K.D.H. Bhadeshia, and D.W. Suh: *Acta Mater.*, 2012, vol. 60, pp. 4085–92.
12. A.W. Thompson and O. Buck: *Met. Trans. A*, 1976, vol. 7A, pp. 329–31.
13. V.M. Shyvaniuk, Y. Mine, and S.M. Teus: *Scr. Mater.*, 2012, vol. 67, pp. 979–82.

14. Y. Mine, Z. Horita, and Y. Murakami: *Acta Mater*., 2009, vol. 57, pp. 2993–3002.
15. J.P. Bressanelli and A. Moskowitz: *Trans. ASM*, 1966, vol. 59, pp. 223–39.
16. C.P. Livitsanos and P.F. Thomson: *Mater Sci. Eng*., 1977, vol. 30, pp. 93–98.
17. D.V. Neff, T.E. Mitchell, and A.R. Troiano: *Trans. ASM*, 1969, vol. 62, pp. 858–68.
18. I. Tamura and T. Maki: *Toward improved ductility toughness*, Climax Molybdenum Development Co (Japan) Ltd., Kyoto, 1972, pp. 183–93.
19. I. Tamura, T. Maki, and H. Hato: *Trans. Iron Steel Inst. Jpn*., 1970, vol. 10, pp. 163–72.
20. J. Talonen: Doctoral Dissertation, Helsinki University, 2007.
21. J. Talonen, P. Nenonen, G. Pape, and H. Hanninen: *Met. Mater. A*, 2005, vol. 36A, pp. 421–31.
22. Y.F. Shen, X.X. Li, X. Sun, Y.D. Wang, and L. Zuo: *Mater. Sci. Eng. A*, 2013, vol. 552, pp. 514–22.
23. S.S. Hecker, M.G. Stout, K.P. Staudhammer, and J.L. Smith: *Met. Trans. A*, 1982, vol. 13A, pp. 619–26.
24. J.A. Lichtenfeld, M.C. Mataya, and C.J. Van Tyne: *Met. Mater. Trans. A*, 2006, vol. 37A, pp. 147–61.
25. A. Kundu and P.C. Chakraborti: *J. Mater. Sci.*, 2010, vol. 45, pp. 5482–89.
26. A.M. Brass and J. Chene: *Corros. Sci*., 2006, vol. 48, pp. 3222–42.
27. J.P. Hirth: *Met. Trans. A*, 1980, vol. 11A, pp. 861–90.
28. H. Matsui, H. Kimura, and S. Moriya: *Mater. Sci. Eng*., 1979, vol. 40, pp. 207–16.
29. C.D. Beachem: *Met. Trans*., 1972, vol. 3, pp. 437–51.
30. D.M. Bromley: Master Thesis, University of British Columbia, 2005.
31. G. Schuster and C.J. Altstetter: *Met. Trans. A*, 1983, vol. 14A, pp. 2085–90.
32. K.J.L. Iyer: *Scr. Met*., 1972, vol. 6, pp. 721–26.
33. K. Tao, H. Choo, H. Li, B. Clausen, J.E. Jin, and Y.K. Lee: *Appl. Phys. Lett*., 2007, vol. 90, pp. 101911-1–3.
34. K.I. Sugimoto, M. Kobayashi, and S.I. Hashimoto: *Met. Trans. A*, 1992, vol. 23A, pp. 3085–91.
35. E.C. Oliver, P.J. Withers, M.R. Daymond, S. Ueta, and T. Mori: *Appl. Phys. A*, 2002, vol. 74, pp. S1143–45.
36. I. Tamura: *Met. Sci*., 1982, vol. 16, pp. 245–53.
37. K. Spencer, J.D. Emburry, K.T. Conlon, M. Veron, and Y. Brechet: *Mater. Sci. Eng. A*, 2004, vol. 387-389, pp. 873–81.
38. G.W. Form and W.M. Baldwin: *Trans ASM*, 1956, vol. 48, pp. 474–85.
39. N.S. Stoloff and R.G. Davies: *Acta Met*., 1964, vol. 12, pp. 473–85.
40. M.J. Marcinkowski and D.S. Miller: *Phil. Mag*., 1961, vol. 6, pp. 871–93.
41. Y.S. Kim, S.S. Kim, D.W. Kim: *Proc. Trans. Korean Nucl. Soc. Spring Meeting*, Korea Nuclear Society, 2011. pp. 857–58.
42. A.H. Cottrell: *In: A Seminar on Relation of Properties to Microstructures*, American Society for Metals, Cleveland, 1954, pp. 131–62.
43. V. Gerold and H.P. Karnthaler: *Acta Met*., 1989, vol. 37, pp. 2177–83.
44. N. Clement, D. Caillard, and J.L. Martin: *Acta Met*., 1982, vol. 32, pp. 961–75.
45. J. Konrad, S. Zaefferer, A. Schneider, D. Raabe, and G. Frommeyer: *Intermetallics*, 2005, vol. 13, pp. 1304–12.
46. P.B. Littlewood: *Phys. Rev. B*, 1986, vol. 34, pp. 1363–66.
47. R.W. Cahn: *Intermetallics*, 1999, vol. 7, pp. 1089–94.
48. A. Marucco and B. Nath: *J. Mater. Sci*., 1988, vol. 23, pp. 2107–14.
49. Y.S. Kim, W.Y. Maeng, and S.S. Kim: *Acta Mater*., 2015, vol. 83, pp. 507–15.
50. T.B. Flanagan, A.P. Craft, T. Kuji, K. Baba, and Y. Sakamoto: *Scr. Met*., 1986, vol. 20, pp. 1745–50.
51. Y. Fukai, Y. Shizuku, and Y. Kurokawa: *J Alloys Compd*., 2001, vol. 329, pp. 195–201.
52. T. Hiroi, Y. Fukai, and K. Mori: *J Alloys Compd*., 2005, vol. 404-406, pp. 252–55.
53. U. Ehrnsten, T. Saukkonen, W. Karlsen, and H. Hanninen: *14th Conf. Env. Mater. Deg. in Nuclear Power Systems*, T. Allen, J. Busby, G. Ilevbare, eds., TMS, VA, 2009, pp. 910–19.
54. M.P. Manahan, R. Kohli, J. Santucci, and P. Sipush: *Nucl. Eng. Des*., 1989, vol. 113, pp. 297–321.
55. S.D. Prokoshkin, L.M. Kaputkina, and M.L. Bernshtein: *Scr. Met*., 1989, vol. 20, pp. 299–304.
56. C. Kaito, Y. Saito, and K. Fujita: *J. Appl. Phys*., 1989, vol. 28, pp. L694–96.
57. A. Chamberod, J. Laugier, and J.M. Penisson: *J. Magn. Magn. Mater*., 1979, vol. 10, pp. 139–44.
58. G. Hausch and H. Warlimont: *Phys. Lett. A*, 1971, vol. 36A, pp. 415–16.
59. G. Hausch and H. Warlimont: *Acta Met*., 1973, vol. 21, pp. 401–13.
60. S. Kachi, Y. Bando, and S. Higuchi: *Jpn. J. Appl. Phys*., 1962, vol. 1, pp. 307–13.
61. N.S. Stoloff and R.G. Davies: *Prog. Mater. Sci*., 1968, vol. 13, pp. 1–84.
62. M.G. Mendiratta, S.K. Ehlers, and H.A. Lipsitt: *Met. Trans. A*, 1987, vol. 18A, pp. 509–18.
63. A. Saha, J. Jung, and G.B. Olson: *J. Comput. Aided Mater. Des*., 2007, vol. 14, pp. 201–33.
64. A.Z. Menshikov, V.E. Arkhipov, A.I. Zakharov, and S.K. Sidorov: *Fiz. Met. Metalloved*., 1972, vol. 34, pp. 309–15.
65. C.B. Post and W.S. Eberly: *Trans. ASM*, 1947, vol. 39, pp. 868–90.